Available online at www.sciencedirect.com
SCIENCE DIRECT®
Journal of Photochemistry and Photobiology A: Chemistry 159 (2003) 135–143
Journal of Photochemistry and Photobiology A:Chemistry
www.elsevier.com/locate/jphotochem

Models of multivinyl free radical photopolymerization kinetics

Tara M. Lovestead [a], Allison K. O'Brien [a], Christopher N. Bowman [a,b,*]

[a] *Department of Chemical Engineering, University of Colorado, Boulder, CO 80309-0424, USA*
[b] *Department of Restorative Dentistry, University of Colorado Health Sciences Center, Denver, CO 80045-0508, USA*

Received 14 January 2003; accepted 28 January 2003

Abstract

Models for predicting multivinyl free radical photopolymerization that incorporate diffusion controlled propagation and termination are discussed. One model focuses on spatial effects by incorporating heat and mass transfer in photopolymerizing films. Temperature, species concentrations, e.g., oxygen and initiator, and light intensity are varied as a function of both time and depth. Specifically, the effect of using polychromatic initiation on oxygen inhibition was investigated. The model predicts that by utilizing initiating radiation of two distinct wavelengths, it is possible to overcome oxygen inhibition and achieve complete cure. The second model incorporates chain length dependent termination (CLDT) and chain transfer to polymer (CTP) in a homogenous, polymerizing system. Specifically, how CTP affects the polymerization rate (R_p), the reaction diffusion coefficient, the scaling relationship between polymerization rate and initiation rate (R_i), i.e., $R_p \propto R_i^{\alpha}$, and the transition from CLDT to reaction diffusion controlled termination was investigated. The model predicts that, in general, at low double bond conversion, CTP inclusion decreases the reaction diffusion coefficient and increases the polymerization rate. Additionally, increasing the CTP rate decreases the double bond conversion both at which the termination mechanism begins to transition from CLDT to reaction diffusion controlled termination and at which reaction diffusion controlled termination becomes the dominant termination mechanism. The model provides more insight into the termination mechanism and complex polymerization behavior.

Keywords: CLDT; Photopolymerization; Simulation; Multivinyl; Oxygen; Chain transfer

1. Introduction

Free radical chain photopolymerizations of multivinyl monomers is advantageous for many reasons, including, the ability to cure rapidly in the absence of a solvent under ambient conditions, flexible monomer chemistry, spatial and temporal control, and the formation of a highly cross-linked network, i.e., a polymer which is insoluble in any organic solvent [1,2]. These remarkable attributes allow for detailed patterning using photomasks [1–5], control of exotherm [6], and the ability to tailor the resulting polymer cross-linking density, degradation rate and mechanism, biocompatibility, and other material properties [7,8]. Additionally, the resulting highly cross-linked network is desirable for applications such as microelectronics [5], protective and decorative coatings [2], orthopedic biomaterials [6,9], drug delivery [8], and dental restorations [10–17].

Multivinyl monomer photopolymerization is a diffusion controlled process due to the almost instantaneous build up of high molecular weight and cross-linked polymer. Since the termination mechanism relies on the diffusivity of radical chains, the termination mechanism becomes mobility restricted at very low double bond conversion, and autoacceleration is observed. Autoacceleration (Fig. 1) is the counterintuitive increase in polymerization rate due to the hindered termination mechanism. This reduced termination causes an increased population of reactive radical chains and a concomitant increase in polymerization rate. The termination mechanism is further complicated by chain length dependencies which have been shown to be important at low to moderate double bond conversion in multivinyl monomer photopolymerizations [18–25].

As more double bonds react, most of the growing radical chains are tethered to the polymer network (Fig. 6b), thus termination occurs by radicals propagating through unreacted vinyl groups until meeting and terminating with another radical. This regime is referred to as reaction diffusion controlled termination and is characterized by the termination event's dependence on the propagation frequency. Eventually, at greater double bond conversion, the propagation mechanism also becomes diffusion controlled and autodeceleration is observed as denoted by the rapid decrease in the polymerization rate. When the reaction is carried out

* Corresponding author. Tel.: +1-303-492-3247; fax: +1-303-492-4341.
E-mail address: christopher.bowman@colorado.edu (C.N. Bowman).

1010-6030/03/$ – see front matter © 2003 Elsevier Science B.V. All rights reserved.
doi:10.1016/S1010-6030(03)00178-3

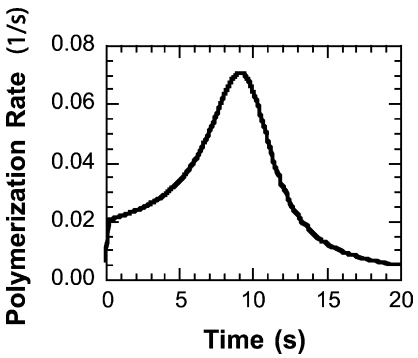

Fig. 1. Polymerization rate vs. time curve for a typical multivinyl photopolymerization is presented and depicts autoacceleration and autodeceleration.

below the glass transition temperature of the final polymer, autodeceleration leads to a limiting double bond conversion that is monomer chemistry and functionality dependent [26].

Increased viscosity and the subsequently decreased diffusion of the reacting species during multivinyl monomer polymerization leads to mass transfer effects [27] and chain length dependent kinetics [18,24,28]. In addition to mobility dependent phenomena, cycle formation [29–31], light attenuation in optically thick samples [6,27,32], non-isothermal effects [6,27], oxygen inhibition [27,33–36], and chain transfer to polymer (CTP) [35–37] also affect the polymerization kinetics. Many of these phenomena lead to polymerization rate, double bond conversion, temperature, and species concentrations that vary spatially within a sample and as a function of conversion.

This array of complex behavior has hindered the attainment of a more complete characterization of multivinyl photopolymerization kinetics. To obtain a better understanding of the photopolymerization mechanism in these systems, two different mathematical models were developed. One model focuses on spatial effects by incorporating heat and mass transfer in photopolymerizing films, where temperature, species concentration, and light intensity are varied as a function of both time and depth. This model specifically investigates the effect of using polychromatic initiation on oxygen inhibition. Additionally, the termination mechanism in multivinyl free radical photopolymerizations is not well understood or characterized, thus, a second model was developed that takes into account chain length dependent termination (CLDT) and CTP in a homogenous polymerizing system. Each model builds upon the general free radical photopolymerization kinetic theory presented below and incorporates diffusion controlled kinetics. An improved understanding of the highly complex termination mechanism, along with the impact of oxygen in photopolymerizing films will further improve efforts to control the multivinyl monomer photopolymerization process, ultimately leading to enhanced polymer properties and increased applications for cross-linked polymers.

2. General free radical photopolymerization kinetic theory

Known cross-linking photopolymerization behavior, such as autoacceleration, autodeceleration, and reaction diffusion, has been incorporated into the fundamental kinetic equations that describe multivinyl free radical photopolymerizations. These models are based on free volume theory and diffusion controlled kinetics [18,38–43].

2.1. Initiation reaction

To model free radical photopolymerizations, accurate predictions of the initiator concentration ([Ab]) and the initiation rate (R_i) are necessary and are described by the following [18,22,24]:

$$\frac{\mathrm{d[Ab]}}{\mathrm{d}t} = \frac{-2.303\varepsilon[\mathrm{Ab}]I\lambda}{N_{\mathrm{Av}}hc} \tag{1}$$

$$R_i = 2\phi I_{\mathrm{a}} = 2\phi\left(\frac{2.303\varepsilon I\lambda[\mathrm{Ab}]}{N_{\mathrm{Av}}hc}\right) \tag{2}$$

In Eq. (1), t is the time, ε the molar absorptivity coefficient, I the incident light intensity in units of power/area, λ the wavelength of the irradiating light, N_{Av} the Avogadro's number, h the Planck's constant, and c the speed of light. For Eq. (2), the 2 arises because, most commonly, two radicals are produced per initiator molecule photocleaving; ϕ is the product of the efficiency and the quantum yield, and I_{a} the photon absorption rate which is evaluated utilizing the Beer–Lambert law [44].

2.2. Propagation and termination

The propagation and termination events are extremely dependent on the reacting species' mobility. Often fractional free volume models are used to describe this relationship between viscosity and the reacting species' mobility. Increased polymer formation (double bond conversion) significantly increases the viscosity (decreases fractional free volume), decreases the mobility, and decreases the ability of a species to propagate and/or terminate. This theory was first applied to monovinyl monomer photopolymerizations [39,40,43,45] with recent application to multivinyl systems [18,38,41,46]. Anseth and Bowman's model utilizes one equation to describe each of the chain length independent propagation and termination kinetic constants [38]. In this model the propagation kinetic constant, k_{p}, is expressed by the following [18,38,42]:

$$k_{\mathrm{p}} = k_{\mathrm{p0}}\left\{1 + \exp\left(A_{\mathrm{p}}\left(\frac{1}{f} - \frac{1}{f_{\mathrm{cp}}}\right)\right)\right\}^{-1} \tag{3}$$

Here, k_{p0} is the propagation kinetic constant at infinite free volume, A_{p} is a constant that controls the onset of autodeceleration and the rate of autodeceleration, and f_{cp} is the

critical free volume at which propagation changes from being chemical reaction controlled to mass transfer controlled. Additionally, k_t is expressed by the following [38,42]:

$$k_t = k_{t0}\left\{1+\left(\exp\left(-A_t\left(\frac{1}{f}-\frac{1}{f_{ct}}\right)\right)+\frac{Rk_p[C{=}C]}{k_{t0}}\right)^{-1}\right\}^{-1} \quad (4)$$

Here, k_{t0} is the termination kinetic constant at infinite free volume, A_t is a constant that controls the onset of autoacceleration and the rate of autoacceleration, and f_{ct} is the critical fractional free volume when termination becomes controlled by the active species' segmental motion. Additionally, R is the reaction diffusion parameter, or the ratio of kinetic constants, $k_t/k_p[C{=}C]$, when reaction diffusion is the dominant termination mechanism [38]. Eqs. (1)–(4) represent the backbone of the free volume based kinetic models presented in this paper that predict multivinyl free radical photopolymerizations.

3. A model of heat and mass transfer effects and spatial effects

3.1. Model development

To simulate a film with variations in temperature, species concentration, and light intensity in the z-direction, heat and mass transfer effects, as well as diffusion controlled propagation and termination are modeled. Heat effects are important because the kinetic constants, as well as the diffusion coefficients, are functions of temperature. Diffusion of small species such as initiator, monomer, primary radical, and oxygen molecules are an important aspect of photopolymerizations, and thus, mass transfer is also critical.

Energy transport has been incorporated into the 1D simulation through an energy balance that includes heat accumulation, heat transfer, and heat generation by reaction and radiation absorption. In the 1D simulation, mass transfer has been incorporated through the addition of a diffusive flux term to the species balance. The general species balance includes species accumulation, diffusive flux, and species consumption or generation by reaction. The energy and species balances have been comprehensively explained by Goodner and Bowman [27] previously.

In the 1D simulation, light attenuation is included utilizing the Beer–Lambert law [44]. The light intensity at depth z (I_z) is described by the following:

$$I_z = I_0 \exp(-\varepsilon c_I z) \quad (5)$$

Here, I_0 is the incident light intensity on the sample, c_I the initiator concentration for a photobleaching initiator or c_I^* (the total initiator concentration for that slice) for a non-photobleaching initiator.

For this particular study, the effect of irradiating with a polychromatic light source is investigated. Specifically, the effect of irradiating with a combination of 254 and 365 nm UV light on thin film systems in inert and oxygen environments is studied. The incident light intensity and initiator and primary radical species balances have been altered appropriately for this study. Distinct relations are written for each wavelength to account for the wavelength dependence of the molar absorptivity of the initiator and monomer. The light intensities of each wavelength at a depth z are described by the following equations:

$$I_{z,365} = I_0 \exp(-\varepsilon_1 c_I z) \quad (6)$$

$$I_{z,254} = I_0 \exp(-\varepsilon_2 c_I z - \varepsilon_3 c_M z) \quad (7)$$

Here, ε_1 and ε_2 are the molar absorptivities of the initiator at 365 and 254 nm, respectively, and ε_3 is the molar absorptivity of the monomer at 254 nm. The initiator and primary radical species balances have been altered such that the initiator is now cleaved by both wavelengths of light, and thus, initiator fragments made by both wavelengths of light form primary radicals.

All parameters used in the model are described by Goodner and Bowman [27], except for the molar absorptivity of 2,2-dimethoxy-2-phenylacetophenone (DMPA) (ε_1 = 345 l/mol cm and ε_2 = 13 000 l/mol cm [47]) and the molar absorptivity of the monomer, 2-hydroxyethyl methacrylate (HEMA) (ε_3 = 63 000 l/mol cm), which was determined experimentally. Additionally, it is assumed that the initiator efficiency is the same at both wavelengths.

3.2. Results and discussion

The effect of irradiating a thin film in air with two wavelengths of light was investigated in this study. The motivation is the inhibition of thin film photopolymerizations by atmospheric oxygen. Oxygen is known to inhibit free radical polymerizations by reacting with initiator, primary, and growing polymer radicals to form peroxy radicals [33,34]. The peroxy radicals are more stable and do not readily reinitiate polymerization, and thus, the oxygen essentially terminates or consumes radicals. If oxygen is present at a low concentration, an induction time will be observed since the polymerization cannot proceed until all of the oxygen is consumed. At higher concentrations, oxygen scavenges all of the radicals in the polymerization, and thus, inhibits or severely retards the polymerization. This effect is most pronounced in thin films, as more oxygen readily diffuses into the sample. In thicker films, the lower depths of the film polymerize, while the top layer remains "tacky" as the oxygen inhibits the reaction at the surface. The unpolymerized top layer reduces surface and optical properties [34]. Several techniques have been utilized to combat the effects of oxygen inhibition. The use of high intensity irradiation sources increases the initiation rate, dramatically increasing the production of primary radicals such that it becomes much greater than their consumption by oxygen. Another alternative is to

polymerize the samples in an inert environment, whereby the oxygen is eliminated from the polymerization [34].

The approach investigated here was to irradiate a sample with two wavelengths of light. The motivation for this was to take advantage of the fact that the molar absorptivity is a function of wavelength. At 365 nm the initiator has a molar absorptivity on the order of 10^2 l/mol cm, while the monomer has negligible absorption. However, below 300 nm, both the initiator and monomer have absorptivities on the order of 10^4 l/mol cm. Thus, at the lower wavelengths, considerable light attenuation will occur due to the high optical density, making these wavelengths non-ideal for photopolymerization. Applying the Beer–Lambert law, it can be calculated that the lower wavelength light will only penetrate about a micron into the sample. However, the large molar absorptivity of the initiator can be utilized to increase the initiation rate, causing the top few microns of the sample to polymerize. The resulting polymer film on top of the sample "caps" off the rapid diffusion of oxygen into the thin film. Once oxygen diffusion into the sample is eliminated, the remaining unpolymerized lower depths of the sample only have to consume the dissolved oxygen to begin the polymerization. The longer wavelength of light, penetrating into the lower depths of the sample, will now polymerize the remainder of the film. Thus, the goal of utilizing the two wavelength initiation scheme is to polymerize thin films in the presence of oxygen, a feat not normally achievable using one wavelength initiation.

First, the effect of the two wavelength initiation on a thin film in an inert atmosphere is shown in Fig. 2. Very early in the polymerization, a large increase in double bond conversion is seen at the top layer in the two wavelength initiated film in comparison to the monochromatic film. However, as the polymerization proceeds, the overall double bond conversion reached in both films is very similar. This result is expected because there are no radical scavenging molecules, such as oxygen.

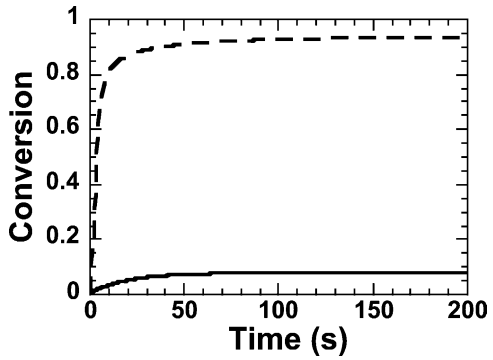

Fig. 3. Double bond conversion as a function of time simulated for a 10 μm film with 5 wt.% DMPA and $I_{365} = 50\,\text{mW/cm}^2$ with no oxygen (– – –) and with 10^{-4} M oxygen (—).

In contrast, Fig. 4 shows the effects of the two wavelength initiation on films in oxygen containing environments, such as air. Usually, a thin film will not appreciably polymerize in air, as shown in Fig. 3. However, with the two wavelength initiation, full polymerization is obtainable. Fig. 4 depicts that the top of the film immediately reaches high conversion, while the rest of the film is negligibly polymerized. However, as the reaction continues, the oxygen is consumed in the lower depths of the sample due to the reduced oxygen diffusivity through the very top layer (Fig. 5). Once the oxygen is consumed, the polymerization proceeds, and nearly complete conversion is achieved.

A good question to ask is whether it is really necessary to have the deep UV radiation since it is at a much higher intensity than the 365 nm light, and instead just increase the intensity of the 365 nm light to that of the 254 nm light. Fig. 4 demonstrates that if $I_{365} = 300\,\text{mW/cm}^2$ and $I_{254} = 0\,\text{mW/cm}^2$, there is still insufficient initiation to overcome the oxygen inhibition. In fact, the 365 nm light source would need to be in excess of $100\,\text{W/cm}^2$ to achieve the same double bond conversion as that seen by polychromatic initiation.

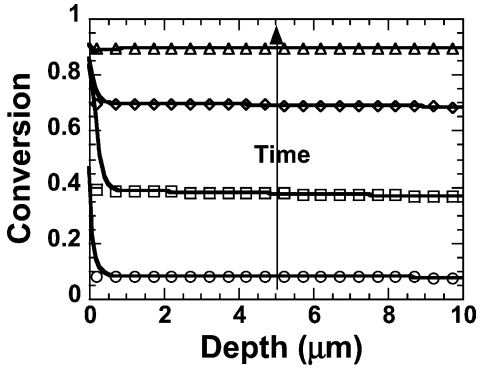

Fig. 2. Double bond conversion as a function of depth for simulated samples exposed to $I_{365} = I_{254} = 50\,\text{mW/cm}^2$ (solid lines) and $I_{365} = 50\,\text{mW/cm}^2$, $I_{254} = 0$ (symbols) for 1, 4, 6, and 35 s. All polymerizations were simulated for a 10 μm film in an inert atmosphere with 5 wt.% DMPA.

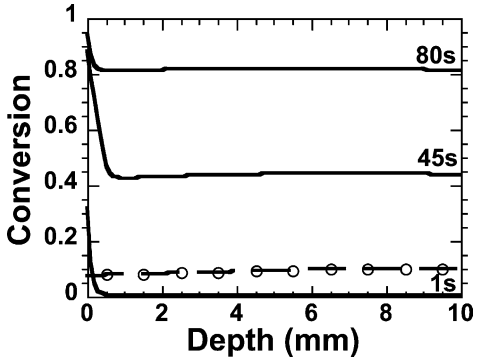

Fig. 4. Double bond conversion as a function of depth for samples simulated with $I_{365} = 50\,\text{mW/cm}^2$ and $I_{254} = 300\,\text{mW/cm}^2$ (—) at various times and with $I_{365} = 300\,\text{mW/cm}^2$ and $I_{254} = 0\,\text{mW/cm}^2$ (○) at its final double bond conversion. All polymerizations were simulated for a 10 μm film with 5 wt.% DMPA, and $[O_2] = 10^{-4}$ M.

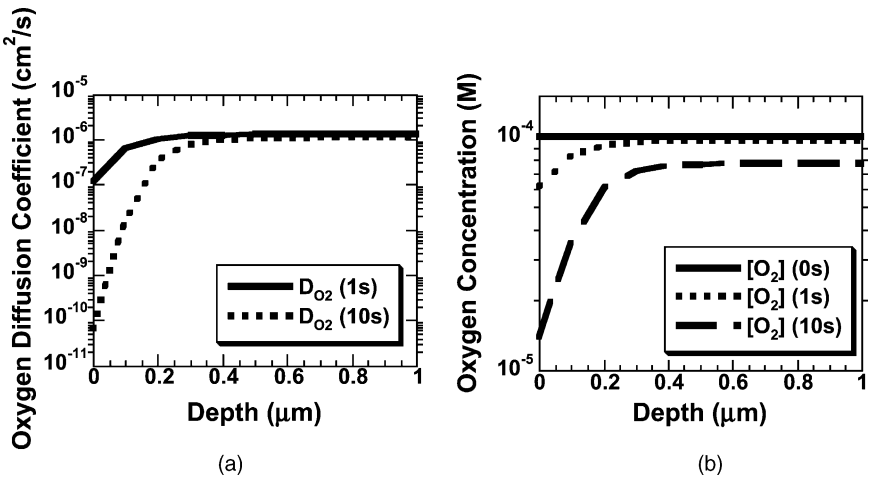

Fig. 5. The diffusivity of oxygen (a) and oxygen concentration (b) as a function of both depth and polymerization time. All polymerizations were simulated for a 10 μm film with 5 wt.% DMPA, $I_{365} = 50\,\text{mW/cm}^2$, $I_{254} = 300\,\text{mW/cm}^2$, and $[O_2] = 10^{-4}$ M.

4. A model of CLDT effects

4.1. Model development

This model simulates a homogenous polymerizing system with variations in polymerization kinetics as a function of both double bond conversion and radical chain mobility. Diffusion controlled propagation and termination, as well as CLDT and CTP are incorporated. Much of what is known about CLDT has been developed for monovinyl diffusion controlled polymerization kinetics [28,39,40,48–63] with Allen and Patrick and Benson and North as two of the first groups to propose a relationship for the dependence of the termination event on the initiation rate. Increasing the initiation rate increases the number of reactive initiator fragments, and thus, radical chains, which increases the termination rate and decreases the average length of the growing radical chains. The shorter chain radicals more readily diffuse through the reaction medium, and thus, more rapidly terminate. The increased termination rate for shorter radical chains decreases the polymerization rate increase expected from the changing initiation rate. Classically, the relationship between polymerization rate and initiation rate is predicted to scale to the 0.5 power, i.e., the scaling exponent, α, is 0.5 for bimolecular, chain length independent termination. This relationship is described by the following:

$$R_p = k_p[C{=}C]\left(\frac{R_i}{2k_t}\right)^{\alpha} \tag{8}$$

In polymerizations where CLDT is important, a less than classical scaling exponent has been predicted and observed. While this is an excepted phenomenon in monovinyl monomer polymerizations, until recently, chain length dependencies have typically been neglected in multivinyl photopolymerizations. Our group [19,20,22–24] and others [21,25] have experimentally studied the effect of changing the light intensity and/or the addition of chain transfer agent on the polymerization of multivinyl monomers. Each work identified a less than classical scaling exponent, i.e., $R_p \propto R_i^{\alpha}$, where $\alpha < 0.5$ at low double bond conversion. Additionally, a CLDT model [18] of multivinyl monomer polymerization was developed. To date, the CLDT model is the only model that is able to predict qualitatively the impact of changing cure conditions on multivinyl photopolymerizations, and subsequently, the less than classical scaling exponent observed experimentally.

In multivinyl polymerizations, CLDT is most important and quantifiable at low conversion when most of the growing radical chains are not tethered to the network and radicals are able to diffuse and terminate at rates relative to their length (Fig. 6a). However, as monomer is converted into polymer, mobility decreases and most of the growing radical chains are tethered to the network. Thus, radicals terminate by reaction diffusion controlled termination, a chain length independent process (Fig. 6b).

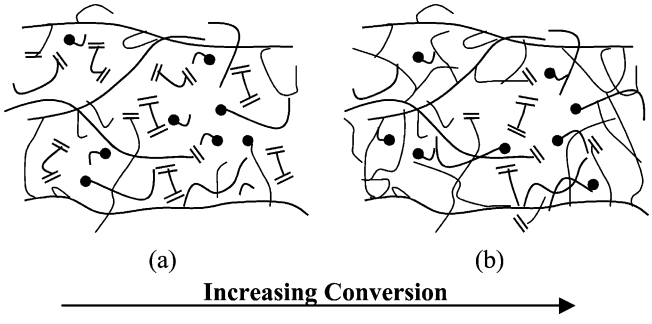

Fig. 6. A schematic of the polymerization reaction at low (a), and high double bond conversion (b) is presented. Early on during the polymerization, monomer and shorter radical chains more readily diffuse and terminate, i.e., CLDT is important. As more double bonds are reacted, the majority of the radicals are tethered to the network; thus, reaction diffusion controlled termination dominates the termination mechanism. Chain length effects are no longer observed in this regime.

The CLDT theory of Benson and North [50] was incorporated as a one-parameter correction to the termination kinetic constant at infinite free volume, k_{t0}, in the mass transfer limited regime. This correction coupled with the previously developed expressions for k_t (Eq. (4)) yields the desired chain length dependent k_{tij} [18,24]:

$$k_{tij} = k_{t110}\left\{1 + \left(\frac{1}{2}\left(\frac{1}{i^{\gamma}} + \frac{1}{j^{\gamma}}\right)\exp\left(-A_t\left(\frac{1}{f} - \frac{1}{f_{ct}}\right)\right) + \frac{Rk_p[C{=}C]}{k_{t110}}\right)^{-1}\right\}^{-1} \quad (9)$$

where γ describes the extent of chain length dependence and is equal to 0.5 based on Random–Walk theory. The model also includes mass balances on the initiator (Eq. (1)), monomer, and radicals of each length (Eqs. (10) and (11))

$$\frac{d[R_1^{\bullet}]}{dt} = R_i - k_p[C{=}C][R_1^{\bullet}] + k_{tp}[DP_1][R^{\bullet}]_{tot} - [R_1^{\bullet}]\sum_{j=1}^{\infty}(k_{tij}[R_j^{\bullet}] + k_{tp}[DP_j]j) \quad (10)$$

$$\frac{d[R_i^{\bullet}]}{dt} = k_p[C{=}C]([R_{i-1}^{\bullet}] - [R_i^{\bullet}]) + k_{tp}[DP_i][R^{\bullet}]_{tot}i - [R_i^{\bullet}]\sum_{j=1}^{\infty}(k_{tij}[R_j^{\bullet}] + k_{tp}[DP_j]j), \quad i > 1 \quad (11)$$

Here, k_{tp} is the polymer chain transfer kinetic constant, $[DP_i]$ the concentration of dead polymer of chain length i, and the propagation kinetic constant is evaluated in Eq. (3). The model parameters are identical to those appearing in a previous publication [18]. The model also predicts $k_{t,avg}$ [18,48,57,64]. The authors acknowledge that the model incorporates several adjustable parameters, but would like to emphasize that the chain length independent model is unable to predict the effects of changing cure conditions on polymerization kinetics. The simple inclusion of CLDT dramatically improves polymerization kinetic predictions for several cure conditions [24].

4.2. Results and discussion

The effects of incorporating CLDT and CTP into the kinetic equations that characterize multivinyl free radical polymerizations of a homogenous sample were investigated in this study. The motivation is improved characterization and understanding of the complex termination mechanism and the overall polymerization behavior in these highly complex systems. Not only is the termination mechanism the least understood aspect of multivinyl photopolymerizations, but also, no model exists today that is able to predict polymerization kinetics for a range of cure conditions. Recently, CLDT was incorporated into the diffusion controlled kinetic equations that describe the termination mechanism and was shown to improve greatly the model's predictive capability when simulating diethylene glycol dimethacrylate (DEGDMA) for several different cure conditions [24]. The initial success of CLDT incorporation revealed the necessity to investigate further the termination mechanism and the role of chain length in multivinyl photopolymerizations. The model presented in this paper further explores CLDT in multivinyl photopolymerizations and also investigates the impact of CTP in these systems.

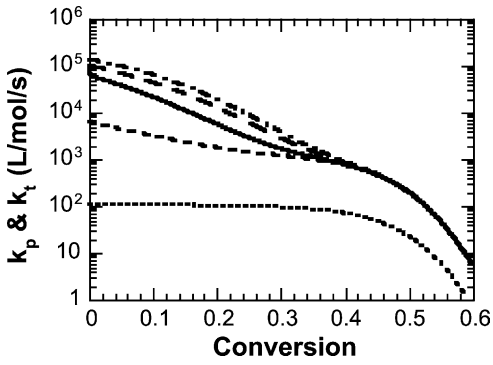

Fig. 7. The simulated kinetic constants ($k_{t,1\_1}$ (–·–), $k_{t,1\_10\,000}$ (– – –), $k_{t,avg}$ (—), $k_{t,10\,000\_10\,000}$ (- - -), and k_p (· · ·)) as a function of both double bond conversion and radical chain length are presented for a typical dimethacrylate polymerization (5 mW/cm^2 with 5 wt.% DMPA).

This model qualitatively predicts the important regimes that typify the complex multivinyl polymerization, such as autoacceleration and autodeceleration (Fig. 1). Accurate prediction of this behavior relies on accurate prediction of the mobility restrictions that impact the kinetic constants. Fig. 7 presents model predictions of the termination kinetic constant as a function of length and double bond conversion, along with an initiation rate dependent $k_{t,avg}$ and the chain length independent k_p, all as functions of double bond conversion. For this dimethacrylate simulation, the termination mechanism is predicted to be diffusion controlled at the onset of polymerization. Thus, CLDT is observed at very low double bond conversion and Eq. (9) predicts that the termination kinetic constant for a radical of unit length terminating with a second, identical radical, $k_{t,1\_1}$, is over 30 times greater than $k_{t,10\,000\_10\,000}$ at about 1% conversion.

The individual k_t's, $k_{t,avg}$, and the differences in termination due to chain length all decrease as monomer is converted to polymer. This decrease represents the polymerization reaction transitioning from a chain length dependent, mass transfer controlled termination mechanism, to a reaction diffusion controlled termination mechanism. Eventually, at around 40% double bond conversion, all of the termination events occur at the same low rate and reaction diffusion dominates the termination reaction as a chain length independent mechanism.

Fig. 7 also reveals the simulation predictions for the propagation kinetic constant. At low to moderate double bond conversion, k_p is not diffusion controlled and very little change in k_p is predicted until about 30% double bond conversion.

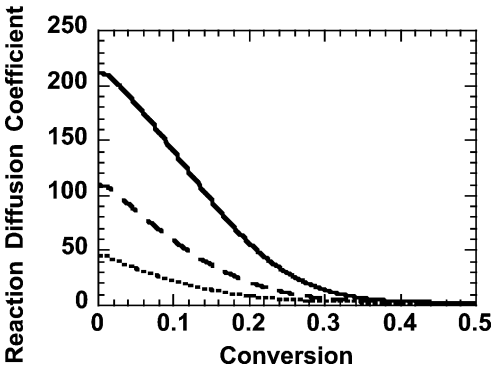

Fig. 8. The reaction diffusion coefficient, R, as predicted by the CLDT model as a function of both double bond conversion and radical chain length ($k_{t,1\_1}$ (—), $k_{t,10\_10}$ (– – –), and $k_{t,100\_100}$ (- - -)). All polymerizations were simulated at 5 mW/cm^2 with 5 wt.% DMPA.

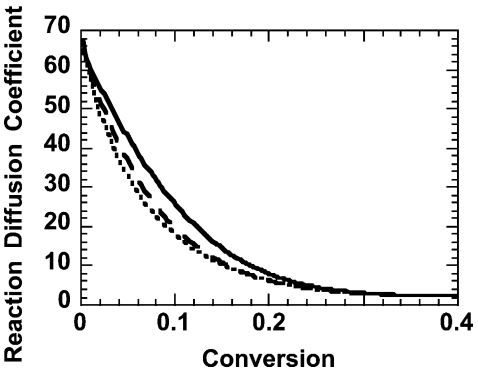

Fig. 9. The reaction diffusion coefficient as predicted by the CLDT model for $k_{t,avg}$ as a function of double bond conversion and the CTP rate (k_{tp} = 0 l/mol s (—), 20 l/mol s (– – –), and 50 l/mol s (· · ·)). All polymerizations were simulated at 5 mW/cm^2 with 5 wt.% DMPA.

Around this conversion, termination is already reaction diffusion controlled, and the propagation mechanism transitions from non-diffusion control to mass transfer, or diffusion, control. At this point, both the termination and propagation kinetic constants are predicted to decrease dramatically.

The transition form CLDT to reaction diffusion controlled termination and the impact of radical chain lengths on this transition are presented in Fig. 8. Reaction diffusion controlled termination is quantified by a plateau in the reaction diffusion coefficient, R, where $R = k_{t,avg}/k_p[C{=}C]$. Thus, when termination no longer occurs as a result of radical chains diffusing through the reaction to meet and terminate, termination is facilitated by radicals propagating through unreacted vinyl groups until meeting and terminating with another radical. Then, the termination kinetic constant is proportional to the propagation frequency, and the reaction diffusion coefficient, R, remains constant. Fig. 8 presents model predictions for R as a function of both radical chain length and double bond conversion. The smaller radical chains are more mobile in the system and more readily terminate at low to moderate double bond conversions, thus, they have a greater R value, where, R = 210, 110, and 44 for $k_{t,1\_1}$ (—), $k_{t,10\_10}$ (– – –), and $k_{t,100\_100}$ (- - -), respectively at the onset of polymerization. Additionally, the double bond conversion where reaction diffusion controlled termination becomes dominant (where R = 2 for DEGDMA) shifts towards greater double bond conversion (40, 44, and 47% double bond conversion) as the radical chain length of the pair of radicals terminating is decreased ($k_{t,100\_100}$ (- - -), $k_{t,10\_10}$ (– – –), and $k_{t,1\_1}$ (—)).

Figs. 7 and 8 reveal a transition from CLDT to reaction diffusion controlled termination, a chain length independent process, during the simulated photopolymerization of the dimethacrylate monomer. This transition from CLDT to reaction diffusion controlled termination is also quantified by evaluating the dependence of polymerization rate on initiation rate, i.e., $R_p \propto R_i^{\alpha}$. Specifically, a deviation from the classically assumed scaling exponent is indicative of the termination kinetic constant having radical chain length dependence.

Berchtold et al. [22–24] examined the effect of changing cure conditions, not only on multifunctional methacrylate monomer photopolymerizations, but also on the corresponding multifunctional acrylate monomer photopolymerizations. In general, the acrylate monomers were less sensitive to conditions designed to impact the kinetic chain length distribution (KCLD), and CLDT was not observed in these systems ($\alpha \geq 0.5$). The lack of ability to impact the KCLD significantly is attributed to increased CTP prevalence in acrylate systems due to the abstractable hydrogens present on the backbone kinetic chains. CTP increases branching, cross-linking, and the polydispersity of the radical chains, and concomitantly shifts the radical chain distribution towards longer radical chains. Since the KCLD is significantly impacted with CTP incorporation, its affect on CLDT and polymerization kinetics was investigated.

CTP was incorporated into the equations that describe the radical chain balances (Eqs. (10) and (11)). A better understanding of both CTP and CLDT provides insight into both the acrylate and methacrylate mechanisms. Specifically, the parameter k_{tp} was manipulated to observe its impact on $k_{t,avg}$, reaction diffusion controlled termination, and the polymerization rate. Additionally, the scaling exponent, α, was investigated to provide insight into the impact of CTP on CLDT and the transition from CLDT to reaction diffusion controlled termination.

Investigating the impact of CTP on the reaction diffusion coefficient provides insight into its effect on $k_{t,avg}$ and, correspondingly, on the KCLD. Model predictions reveal that increasing the CTP rate decreases R at low to moderate conversions (Fig. 9). This decrease is attributed to the increased population of longer chain radicals. Deviations from the model prediction of R without CTP occur at less than 2% conversion for both CTP rates. Also, increasing the CTP rate (k_{tp} = 0 l/mol s (—), 20 l/mol s (– – –), and 50 l/mol s (· · ·))

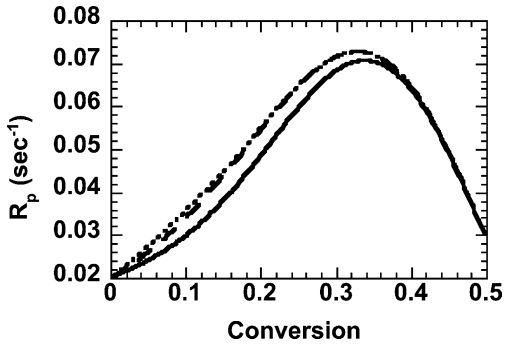

Fig. 10. The impact of increasing the CTP rate (k_{tp} = 0 l/mol s (—), 20 l/mol s (– – –), and 50 l/mol s (· · ·)) on the polymerization rate as a function of double bond conversion is presented. All polymerizations were simulated at 5 mW/cm^2 with 5 wt.% DMPA.

was shown to decrease the conversion at which reaction diffusion controls termination. This prediction makes sense due to the increased concentration of less mobile, longer radical chains.

The effect of increasing the longer radical chain concentration is also observed by predicting the polymerization rate with increasing CTP rate (Fig. 10). At low to moderate conversions, the polymerization rate is observed to increase with increasing CTP due to the overall decrease in termination, and concomitant increase in the longer radical chain concentration. Additionally, the maximum polymerization rate was increased with increasing CTP rate (R_p = 0.071, 0.073, and 0.073 s^{-1} for k_{tp} = 0 l/mol s (—), 20 l/mol s (– – –), and 50 l/mol s (· · ·), respectively).

Valuable information about the polymerization kinetics is also obtained by examining the impact of CTP on the scaling exponent, α. In all of the simulations at low double bond conversion, α is observed to deviate significantly from the classically predicted scaling exponent of 0.5, where α is less than 0.5 for the majority of the polymerization before reaction diffusion controlled termination. This behavior is expected for systems where termination is chain length dependent.

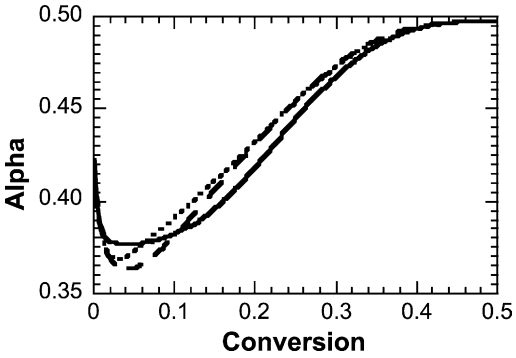

Fig. 11. The scaling exponent, α, that describes the relationship between polymerization rate and initiation rate, i.e., $R_p \propto R_i^{\alpha}$ as predicted by the CLDT model is presented as a function of double bond conversion and CTP addition (k_{tp} = 0 l/mol s (—), 20 l/mol s (– – –), and 50 l/mol s (· · ·)). All polymerizations were simulated at 5 mW/cm^2 with both 0.1 and 5 wt.% DMPA.

As the double bond conversion increases, the CLDT regime transitions to the classical, chain length independent regime, where reaction diffusion controlled termination is the dominant termination mechanism, and a plateau at α = 0.5 is observed for all simulations. Increasing CTP rate decreases α at low double bond conversion and decreases the double bond conversion both where the transition from CLDT to reaction diffusion controlled termination begins, and where reaction diffusion controlled termination becomes the dominant termination mechanism as determined from the plateau of α = 0.5 (Fig. 11).

5. Conclusions

Two models of multivinyl free radical photopolymerization that utilize free volume theory are presented with the goal of attaining a better understanding of the complex multivinyl free radical photopolymerization reaction. Both models incorporate diffusion controlled propagation and termination. The first models temperature, species concentrations, and light intensity variation as a function of both time and depth. This model was applied to predict the effects of polychromatic initiation on oxygen inhibition of thin films. The goal was to photopolymerize thin films in the presence of oxygen, a feat not normally achievable using monochromatic light. The motivation for the polychromatic initiation was to take advantage of the fact that the molar absorptivity of the initiator is two orders of magnitude greater in the deep UV range, and thus, very rapid initiation is possible at the top of the sample. It was found for a 10 μm film with 10^{-4} M oxygen, using polychromatic initiation of I_{254} = 300 mW/cm^2 and I_{365} = 50 mW/cm^2, complete double bond conversion was achieved in about 1 min. Additionally, a CLDT model was expanded to include CTP. Studying how CTP affects the reaction diffusion coefficient, the polymerization rate, the relationship between polymerization rate and initiation rate, and the transition from CLDT to reaction diffusion controlled termination provides more insight into the termination mechanism and complex polymerization behavior. In general, at low conversion, increasing CTP rate decreases the reaction diffusion coefficient, increases the polymerization rate, and increases the importance of CLDT. Additionally, increasing the CTP rate decreases the conversion both at which the termination mechanism begins to transition from CLDT to reaction diffusion controlled termination and at which reaction diffusion controlled termination becomes the dominant termination mechanism. The two models presented in this paper provide insight into phenomena that occur in complex multivinyl photopolymerizations.

Acknowledgements

The authors thank the IUCRC for Fundamentals and Applications of Photopolymerizations, and the Department of

Education for granting a GAANN fellowship to TML and AKO.

References

[1] C. Decker, J. Coat. Technol. 59 (1987) 97–106.
[2] C. Decker, Acta Polym. 45 (1994) 333–347.
[3] N. Luo, J. Hutchison, K. Anseth, C. Bowman, Macromolecules 25 (2002) 2487–2493.
[4] N. Luo, J. Hutchison, K. Anseth, C. Bowman, J. Polym. Sci. A 40 (2002) 1885–1891.
[5] J.G. Kloosterboer, Adv. Polym. Sci. 84 (1988) 1–61.
[6] J.A. Burdick, A.J. Peterson, K.S. Anseth, Biomaterials 22 (2001) 1779–1786.
[7] K.S. Anseth, D.J. Quick, Macromol. Rapid Commun. 22 (2001) 564–572.
[8] K.S. Anseth, A.T. Metters, S.J. Bryant, P.J. Martens, J.H. Elisseeff, C.N. Bowman, J. Control. Release 78 (2002) 199–209.
[9] A.K. Burkoth, K.S. Anseth, Macromolecules 32 (1999) 1438–1444.
[10] L.G. Lovell, K.A. Berchtold, J.E. Elliott, H. Lu, C.N. Bowman, Polym. Adv. Technol. 12 (2001) 335–345.
[11] K.S. Anseth, S.M. Newman, C.N. Bowman, Adv. Polym. Sci. 122 (1995) 177–217.
[12] J.E. Elliott, L.G. Lovell, C.N. Bowman, Dental Mater. 17 (2001) 221–229.
[13] K.A. Berchtold, J.W. Stansbury, C.N. Bowman, J. Dental Res. 79 (2000) 32.
[14] H. Lu, L.G. Lovell, C.N. Bowman, Macromolecules 34 (2001) 8021–8025.
[15] L.G. Lovell, H. Lu, J.E. Elliott, J.W. Stansbury, C.N. Bowman, Dental Mater. 17 (2001) 504–511.
[16] L.G. Lovell, J.W. Stansbury, C.N. Bowman, J. Dental Res. 79 (2000) 33.
[17] L.G. Lovell, J.W. Stansbury, D.C. Syrpes, C.N. Bowman, Macromolecules 32 (1999) 1321–3913.
[18] T.M. Lovestead, K.A. Berchtold, C.N. Bowman, Macromol. Theory Simul. 11 (2002) 729–738.
[19] B. Hacioglu, K.A. Berchtold, L.G. Lovell, J. Nie, C.N. Bowman, Biomaterials 23 (2002) 4057–4064.
[20] K.S. Anseth, L.M. Kline, T.A. Walker, K.J. Anderson, C.N. Bowman, Macromolecules 28 (1995) 2491–2499.
[21] W.D. Cook, J. Polym. Sci. A 31 (1993) 1053–1067.
[22] K.A. Berchtold, B. Hacioglu, L. Lovell, J. Nie, C.N. Bowman, Macromolecules 34 (2001) 5103–5111.
[23] K.A. Berchtold, L.G. Lovell, J. Nie, B. Hacioglu, C.N. Bowman, Polymer 42 (2001) 4925–4929.
[24] K.A. Berchtold, T.M. Lovestead, C.N. Bowman, Macromolecules 35 (2002) 7968–7975.
[25] W.D. Cook, Polymer 33 (1992) 600–609.
[26] S.K. Soh, D.C. Sundberg, J. Polym. Sci., Polym. Chem. Ed. 20 (1982) 1299–1313.
[27] M.D. Goodner, C.N. Bowman, Chem. Eng. Sci. 57 (2002) 887–900.
[28] S. Zhu, A.E. Hamielec, Macromolecules 22 (1989) 3093–3098.
[29] J.E. Elliott, C.N. Bowman, Macromolecules 32 (1999) 8621–8628.
[30] J.E. Elliott, C.N. Bowman, Macromolecules 34 (2001) 4642–4649.
[31] J.E. Elliott, J.W. Anseth, C.N. Bowman, Chem. Eng. Sci. 56 (2001) 3173–3184.
[32] J.A. Burdick, T.M. Lovestead, K.S. Anseth, Biomacromolecules 4 (2003) 149–156.
[33] C. Decker, J. Faure, M. Fizet, L. Rychla, Photogr. Sci. Eng. 23 (1979) 137–140.
[34] C. Decker, A.D. Jenkins, Macromolecules 18 (1985) 1241–1244.
[35] J.G. Kloosterboer, G.F.C.M. Liften, Polym. Commun. 28 (1987) 2–5.
[36] J.G. Kloosterboer, G.F.C.M. Lijten, F.J.A.M. Greidanus, Polym. Rep. 27 (1986) 268–271.
[37] J.G. Kloosterboer, G.F.C.M. Lijten, in: R.A. Dickie, S.S. Labana, R.S. Bauer (Eds.), ACS Symposium Series 367, American Chemical Society, Washington, DC, 1988, pp. 409–426.
[38] K.S. Anseth, C.N. Bowman, Polym. React. Eng. 1 (1992–1993) 4520–4999.
[39] S.K. Soh, D.C. Sundberg, J. Polym. Sci., Polym. Chem. Ed. 20 (1982) 1299–1313.
[40] S.K. Soh, D.C. Sundberg, J. Polym. Sci., Polym. Chem. Ed. 20 (1982) 1315–1329.
[41] C.N. Bowman, N.A. Peppas, Macromolecules 24 (1991) 1914–1920.
[42] M.D. Goodner, H.R. Lee, C.N. Bowman, Ind. Eng. Chem. Res. 36 (1997) 1247–1252.
[43] F.L. Marten, A.E. Hamielec, J. Appl. Polym. Sci. 27 (1982) 489–505.
[44] G. Odian, Principles of Polymerization, 3rd ed., Wiley, New York, 1991.
[45] F. Bueche, Physical Properties of Polymers, Interscience, London, 1962.
[46] M. Wen, A.V. McCormick, Macromolecules 33 (2000) 9247–9254.
[47] C.G. Roffey, Photogeneration of Reactive Species for UV Curing, John Wiley & Sons, West Sussex, England, 1997.
[48] G.T. Russell, R.G. Gilbert, D.H. Napper, Macromolecules 25 (1992) 2459–2469.
[49] J.N. Cardenas, K.F. O'Driscoll, Polym. Chem. Ed. 14 (1976) 883–897.
[50] S.W. Benson, A.M. North, J. Am. Chem. Soc. 84 (1962) 935–940.
[51] O.F. Olaj, G. Zifferer, A. Kornherr, Macromol. Theory Simul. 7 (1998) 321–326.
[52] G. Russell, Aust. J. Chem. 55 (2002) 399–414.
[53] H. Tobita, Macromolecules 28 (1995) 5119–5127.
[54] P.A.G.M. Scheren, G.T. Russell, D.F. Sangster, R.G. Gilbert, A.L. German, Macromolecules 28 (1995) 3637–3649.
[55] O.F. Olaj, A. Kornherr, G. Zifferer, Macromol. Theory Simul. 9 (2000) 131–140.
[56] O.F. Olaj, A. Kornherr, P. Vana, M. Zoder, G. Zifferer, Macromol. Symp. 182 (2002) 15–30.
[57] P.E.M. Allen, C.R. Patrick, Macromol. Chem. 47 (1961) 154–167.
[58] G.T. Russell, Macromol. Theory Simul. 3 (1994) 439–468.
[59] H. Mahabadi, Macromolecules 24 (1991) 606–609.
[60] G.A. O'Neil, J.M. Torkelson, Macromolecules 32 (1999) 411–422.
[61] G.T. Russell, Macromol. Theory Simul. 4 (1995) 549–576.
[62] G.I. Litvinenko, V.A. Kaminsky, Prog. React. Kinetics 19 (1994) 139–193.
[63] A.N. Nikitin, A.V. Evseev, Macromol. Theory Simul. 6 (1997) 1191–1210.
[64] H. Mahabadi, Macromolecules 18 (1985) 1319–1324.